

Synthesis and Structural Characterization of Heteroboroxines with MB₂O₃ Core (M = Sb, Bi, Sn)

Barbora Mairychová,[†] Tomáš Svoboda,[†] Petr Štěpnička,[‡] Aleš Růžička,[†] Remco W. A. Havenith,[§] Mercedes Alonso,^{||} Frank De Proft,^{*,||} Roman Jambor,^{*,†} and Libor Dostál^{*,†}

[†]Department of General and Inorganic Chemistry, Faculty of Chemical Technology, University of Pardubice, Studentská 573, Pardubice 53210, Czech Republic

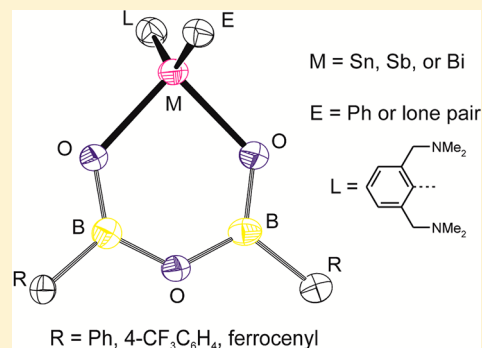
[‡]Department of Inorganic Chemistry, Faculty of Science, Charles University in Prague, Hlavova 2030, CZ-12840 Prague, Czech Republic

[§]Theoretical Chemistry, Zernike Institute for Advanced Materials, University of Groningen Nijenborgh 4, 9747 AG Groningen, The Netherlands

^{||}Eenheid Algemene Chemie (ALGC), Vrije Universiteit Brussel (VUB), Pleinlaan 2, B-1050 Brussels, Belgium

Supporting Information

ABSTRACT: Reaction of organoantimony and organobismuth oxides (LSbO)₂ and (LBiO)₂ (where L is [2,6-bis(dimethylamino)methyl]phenyl) with four equivalents of the organoboronic acids gave new heteroboroxines LM[(OBR)₂O] **1a–2c** (for M = Sb: R = Ph (**1a**), 4-CF₃C₆H₄ (**1b**), ferrocenyl (**1c**); for M = Bi: R = Ph (**2a**), 4-CF₃C₆H₄ (**2b**), and ferrocenyl (**2c**)). Analogously, reaction between organotin carbonate L(Ph)Sn(CO₃) and two equivalents of organoboronic acids yielded compounds L(Ph)Sn[(OBR)₂O] (where R = Ph (**3a**), 4-CF₃C₆H₄ (**3b**), and ferrocenyl (**3c**)). All compounds were characterized by elemental analysis and NMR spectroscopy. Their structure was described both in solution (NMR studies) and in the solid state (X-ray diffraction analyses **1a**, **1c**, **2b**, **3b**, and **3c**). All compounds contain a central MB₂O₃ core (M = Sb, Bi, Sn), and the bonding situation within these rings and their potential aromaticity was investigated by the help of computational methods.



INTRODUCTION

Boroxines are well-known species, readily accessible by dehydration of the corresponding organoboronic acids.¹ Recently, the chemistry of these compounds featuring six-membered boroxine rings has undergone a period of renaissance due to potential applications in material science.² In 2005, Yaghi and co-workers reported the first crystalline boroxine covalent organic framework (COF),³ a landmark in the boroxine chemistry. Since this disclosure, many COF-related materials have emerged, which significantly expanded the interest in material properties of boroxines.⁴ Consequently, boroxines were studied as high-performance polymer electrolytes,⁵ flame retardants,² materials for nonlinear optics,⁶ reactants or catalysts for various organic transformation,⁷ and Lewis acids for formation of adducts with N-donor molecules.⁸ Substitution of the central B₃O₃ core with ferrocene moieties in turn allowed isolation of redox-active boroxines.⁹ Nevertheless, the chemistry of heteroboroxines, in which one of the boron atoms is substituted by a heteroatom M to form a MB₂O₃ six-membered ring, remains nearly unexplored, as recently pointed out by Korich and Iovine.^{2a} Compounds L'Al[(OBR)₂O] (where L' = HC(CMeNAr)₂, Ar = 2,6-*i*-PrC₆H₃, and R = Ph, 3-MeC₆H₄, 3-FC₆H₄), prepared by the reactions between the

aluminum(I) compound L'Al or the hydride L'AlH₂ and the corresponding arylboronic acid, represent prominent examples of such compounds.¹⁰ Molecular borasiloxanes with the Si₂B₂O₄ eight-membered ring were also reported.¹¹ Structurally characterized organotin(IV) compounds Sn(*t*-Bu)₂[OB(OH)Ph]₂, Sn(*t*-Bu)₂(OH)₂[(*t*-Bu)₂SnO]₂OBC₆H₂Me₃-2,4,6]₂·2MeCN,¹² and organophosphorus(V) compounds¹³ stabilized by Salen-type ligand are other rare examples of compounds bearing a heteroboroxine motif in the structure. In a continuation of our investigations into main group organometallic oxides,¹⁴ we report herein a straightforward synthesis of hitherto unknown heteroboroxines LM[(OBR)₂O] and L(Ph)Sn[(OBR)₂O], where M = Sb and Bi, L = [2,6-bis(dimethylamino)methyl]phenyl, R = Ph, 4-CF₃C₆H₄, and ferrocenyl, comprising MB₂O₃ six-membered rings, from oxides (LSbO)₂ and (LBiO)₂ or organotin carbonate L(Ph)Sn(CO₃) and the corresponding organoboronic acids. All compounds were characterized by elemental analysis and multinuclear NMR spectroscopy. The bonding situation within the central

Received: October 3, 2012

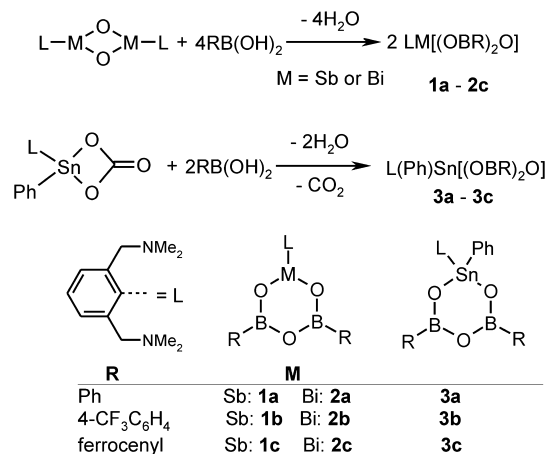
Published: January 17, 2013

MB₂O₃ rings as well as their aromaticity has been investigated by computational methods.

RESULTS AND DISCUSSION

Treatment of intramolecularly coordinated organoantimony and organobismuth oxides (LSbO)₂^{14a} and (LBiO)₂^{14b} with four equivalents of the corresponding organoboronic acids smoothly provided heteroboroxines **1a–c** and **2a–c**, respectively (Scheme 1). Complete deprotonation of the starting boronic acids was confirmed by IR spectra, lacking characteristic vibrations due to the B–OH moieties.

Scheme 1. Preparation of Compounds **1a–3c**



¹H NMR spectra of **1a–2c** revealed the signals of the ligand L and groups R in a mutual ratio of 1:2 and further showed an AX pattern for methylene CH₂N and two signals for the NMe₂ groups in L. The observed patterns suggest the presence of N→M interactions in **1a–2c** with a pseudofacial coordination of the CH₂NMe₂ arms to the central atom M. One set of signals was observed for the substituents R on the heteroboroxine ring (including the ferrocenyl moieties in **1c** and **2c**) in the ¹H and ¹³C NMR spectra, indicating their equivalency in solution.

The formulation of **1a–2c** was unambiguously corroborated by X-ray diffraction analysis. Suitable single crystals of **1a**, **1c**, and **2b** were obtained from saturated toluene solutions at room temperature. The molecular structures of **1a**, **1c**, and **2b** together with the relevant structural parameters are depicted in Figures 1, 2, and 3, respectively.

The central Sb and Bi atoms are stabilized by coordination of the NCN pincer-type ligand. The bond lengths of the M–N bonds (M = Sb: 2.621(3)–2.798(4), M = Bi: 2.671(5) Å) indicate the presence of significant N→M intramolecular interactions in all compounds. Coordination of the ligand L may be described as pseudo-facial as indicated by the N–M–N angles, which fall within a narrow range 118.48(14)–119.90(8)°. The coordination polyhedron around the antimony and bismuth atoms in **1a**, **1c**, and **2b** is completed by two oxygen atoms from the boronic acid residues and is best described as a strongly distorted tetragonal pyramid with the ipso-carbon atom C1 located in the apical position. The values of two M–O bond distances within each central heteroboroxine ring are similar (2.042(2) and 2.0565(19) Å for **1a**, 2.181(4) Å for **2b**, 2.041(2) and 2.034(2) Å for **1c**), suggesting M–O covalent bonding (Σ_{cov}(M, O) = 2.03 Å (Sb), 2.14 Å (Bi)).¹⁵

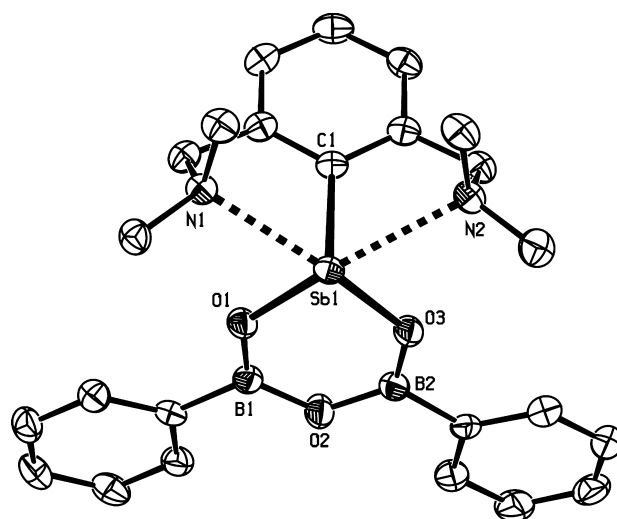


Figure 1. Molecular structure of **1a**; hydrogen atoms omitted for clarity. Selected bond lengths [Å] and angles [degrees]: Sb(1)–C(1) 2.155(3), Sb(1)–N(1) 2.759(3), Sb(1)–N(2) 2.798(4), Sb(1)–O(1) 2.042(2), Sb(1)–O(3) 2.0565(19), B(1)–O(1) 1.334(4), B(1)–O(2) 1.387(4), B(2)–O(2) 1.381(4), B(2)–O(3) 1.334(4), O(1)–Sb(1)–O(3) 86.07(8), O(1)–B(1)–O(2) 123.8(3), O(2)–B(2)–O(3) 124.7(3), Sb(1)–O(1)–B(1) 130.11(19), B(1)–O(2)–B(2) 125.8(3), B(1)–O(3)–Sb(1) 128.99(19).

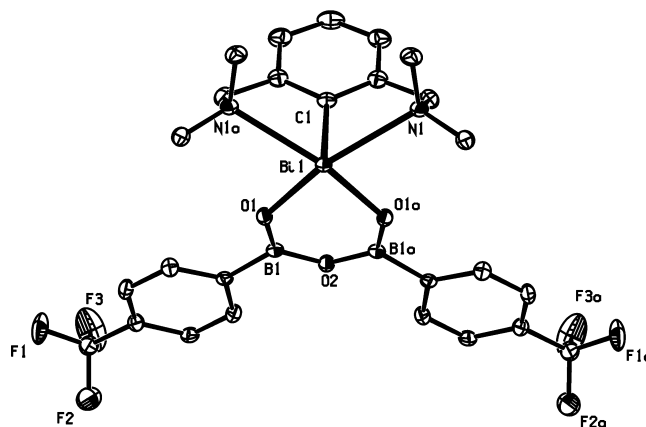


Figure 2. Molecular structure of **2b**; hydrogen atoms omitted for clarity. Selected bond lengths [Å] and angles [degrees]: (**2b**, symmetry operator $a = x, 1/2 - y, z$): Bi(1)–C(1) 2.234(8), Bi(1)–N(1) 2.671(5), Bi(1)–O(1) 2.181(4), B(1)–O(1) 1.326(7), B(1)–O(2) 1.378(7), O(1)–Bi(1)–O(1a) 83.76(14), O(1)–B(1)–O(2) 126.1(6), Bi(1)–O(1)–B(1) 127.1(4), B(1)–O(2)–B(2) 126.6(5).

Reactions of organotin carbonate L(Ph)Sn(CO₃)^{14c} with two equivalents of the respective organoboronic acid provided analogous organotin boroxines **3a–c** (Scheme 1). IR spectra of the crude reaction mixtures showed no vibrations due to B–OH, thereby proving complete deprotonation of the starting boronic acids.

¹H NMR spectra of **3a–c** again confirmed the presence of the ligand L and groups R in a 1:2 ratio. Besides, the spectra revealed an AX spin system due to methylene CH₂N and one broad signal for the NMe₂ groups of the ligand L, suggesting the presence of N→Sn interaction with pseudofacial coordination of CH₂NMe₂ arms of the ligand L to the central tin atom. An equivalency of substituents R on the heteroboroxine ring was proven by the ¹H and ¹³C NMR spectra, where only one set of signals was observed. ¹¹⁹Sn NMR spectra displayed single

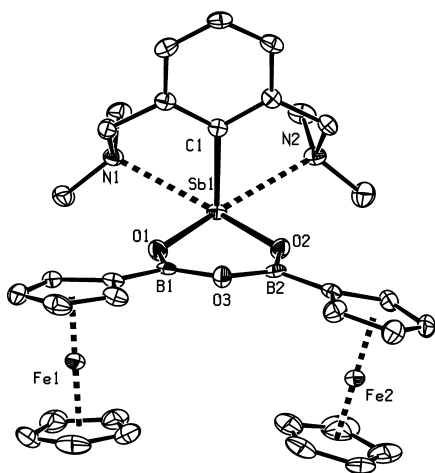


Figure 3. Molecular structure of **1c**; hydrogen atoms omitted for clarity. Selected bond lengths [Angstroms] and angles [degrees]: Sb(1)–C(1) 2.164(3), Sb(1)–N(1) 2.670(3), Sb(1)–N(2) 2.621(3), Sb(1)–O(1) 2.041(2), Sb(1)–O(3) 2.034(2), B(1)–O(1) 1.340(4), B(1)–O(3) 1.386(4), B(2)–O(2) 1.346(4), B(2)–O(3) 1.383(4), O(1)–Sb(1)–O(3) 85.84(9), O(1)–B(1)–O(2) 123.7(3), O(2)–B(2)–O(3) 124.0(3), Sb(1)–O(1)–B(1) 128.2(2), B(1)–O(3)–B(2) 125.4(3), Sb(1)–O(2)–B(2) 128.7(2).

resonances at $\delta = -359.1$ ppm for **3a**, $\delta = -364.0$ ppm for **3b**, and at $\delta = -358.0$ ppm for **3c**, which is indeed consistent with the presence of hexacoordinated tin atoms.¹⁶

Single crystals of **3b** and **3c** were obtained from saturated toluene solution at room temperature and subjected to X-ray diffraction analysis. Views of the molecular structures are presented in Figures 4 (**3a**) and 5 (**3c**) along with selected structural parameters.

In both compounds **3b** and **3c**, the tin center is coordinated by two nitrogen atoms (N–Sn distances in the range of 2.574(3)–2.727(3) Å) in a pseudofacial fashion as demonstrated by the angles N–Sn–N 118.36(13)° for **3b** and 118.58(9)° for **3c**. The geometry of the central tin atom can be

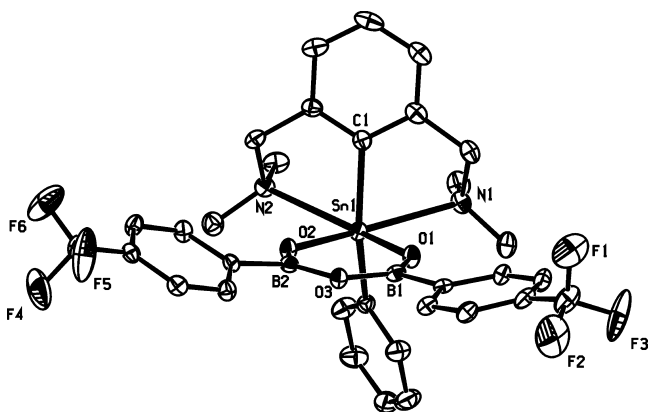


Figure 4. Molecular structure of **3b**; hydrogen atoms omitted for clarity. Selected bond lengths [Angstroms] and angles [degrees]: Sn(1)–C(1) 2.105(5), Sn(1)–C(13) 2.122(5), Sn(1)–N(1) 2.582(4), Sn(1)–N(2) 2.716(4), Sn(1)–O(1) 2.044(3), Sn(1)–O(2) 2.046(3), B(1)–O(1) 1.335(6), B(1)–O(3) 1.385(6), B(2)–O(2) 1.333(6), B(2)–O(3) 1.385(6), O(1)–Sn(1)–O(2) 88.39(13), O(1)–B(1)–O(3) 124.5(4), O(2)–B(2)–O(3) 124.6(4), Sn(1)–O(1)–B(1) 127.8(3), Sn(1)–O(2)–B(2) 127.4(3), B(1)–O(3)–B(2) 126.8(4).

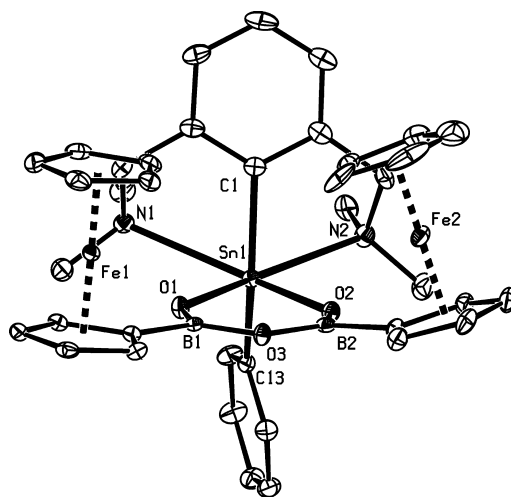


Figure 5. Molecular structures of **3c**; hydrogen atoms omitted for clarity. Selected bond lengths [Angstroms] and angles [degrees]: Sn(1)–C(1) 2.115(3), Sn(1)–C(13) 2.123(3), Sn(1)–N(1) 2.727(3), Sn(1)–N(2) 2.574(3), Sn(1)–O(1) 2.032(2), Sn(1)–O(2) 2.035(2), B(1)–O(1) 1.332(4), B(1)–O(3) 1.394(4), B(2)–O(2) 1.339(4), B(2)–O(3) 1.390(4), O(1)–Sn(1)–O(2) 88.75(9), O(1)–B(1)–O(3) 124.5(3), O(2)–B(2)–O(3) 124.4(3), Sn(1)–O(1)–B(1) 127.2(2), Sn(1)–O(2)–B(2) 126.5(2), B(1)–O(3)–B(2) 126.3(3).

described as distorted octahedral. The Sn–O bond distances (2.032(2)–2.046(3) Å) within the heteroboroxine ring again indicate formation of Sn–O covalent bonds ($\Sigma_{\text{cov}}(\text{Sn}, \text{O}) = 2.03$).¹⁵

It is noteworthy that all structures of **1a**, **1c**, **2b**, **3b**, and **3c** contain the central MB_2O_3 ring system, where both B–O(M) bonds are slightly shorter (1.326(7)–1.346(4) Å) than the remaining B–O(B) bonds (1.378(7)–1.394(4) Å) and also shorter than the B–O distances in the corresponding boroxines $\text{R}_3\text{B}_3\text{O}_3$.^{17,9d} All values are, however, still slightly shorter than the sum of the covalent radii $\Sigma_{\text{cov}}(\text{B}, \text{O}) = 1.48$ Å.¹⁵ The presence of the heteroatom M leads also to a significant distortion of the central six-membered ring as demonstrated by the values of the O–B–O (123.8(3)–127.3(3)° in **1a**, **1c**, **2b**, **3b**, and **3c**), B–O–B (125.4(3)–126.8(4)°), and M–B–O angles (126.5(2)–130.11(19)°), which are significantly wider than the ideal value of 120° observed usually for simple boroxines such as $\text{Ph}_3\text{B}_3\text{O}_3$ ¹⁷ or $\text{Fc}_3\text{B}_3\text{O}_3$.^{9d} This distortion is also reflected in acute O–M–O angles (86.07(8)° **1a**, 83.76(14)° **2b**, 88.39(13)° **3b**, 85.84(9)° **1c**, 88.39(13)° **3c**). The presence of heteroatom M is further reflected in a distortion of the MB_2O_3 rings from planarity. Atoms M are slightly displaced from the mean plane of the B_2O_3 moiety, distances of M from this plane being 0.165 (**1a**), 0.423 (**1c**), 0.411 (**2b**), 0.071 (**3b**), and 0.253 (**3c**) Å. The ligand L is oriented nearly perpendicularly to the MB_2O_3 ring system in all structurally characterized compounds.

The most striking feature regarding the substituents on the heteroboroxine rings is the position of the ferrocenyl moieties in **1c** and **3c**. While in the case of **1c** the ferrocenyl residues are placed on the opposite side (anti) of the heteroboroxine ring with respect to L, those in **3c** are directed toward ligand L (i.e., in syn fashion). In the case of the triferrocenylboroxine, the ferrocenyl moieties are also oriented in all-syn fashion.^{9d} Structures of all possible isomers of **1c**, **2c**, and **3c** (all-syn, all-anti, and anti-syn) were optimized by DFT methods and

Table 1. GIAO-B3LYP/cc-pVDZ^b//B3LYP/cc-pVDZ^b Computed NICS for Heteroboroxines Reported in This Work: Model Compounds 1, 2, and 3 and Parent Boroxine H₃B₃O₃^a

molecule	NICS(0)	NICS(1) ^c	NICS(-1) ^c	NICS _{zz} (0) ^d	NICS _{zz} (1) ^d	NICS _{zz} (-1) ^d	σ _{ip} ^e
1 ^f	0.1	0.6	0.1	25.7	5.2	5.0	-12.7
1a	1.2	0.8	0.9	28.1	9.0	7.2	-12.3
1b	1.1	0.8	0.8	27.9	9.0	7.2	-12.3
1c	0.7	0.1	0.9	26.8	7.4	7.7	-12.3
2 ^f	-0.6	0.3	-0.2	24.7	5.6	4.2	-13.2
2a	1.1	0.7	0.9	27.8	9.2	7.5	-12.3
2b	1.1	0.7	0.8	27.7	9.3	7.5	-12.2
2c	0.8	0.3	1.0	27.0	8.2	8.2	-12.3
3 ^f	0.0	0.1	0.1	25.9	5.0	5.0	-12.9
3a	1.4	0.8	1.2	29.1	9.2	7.9	-12.5
3b	1.4	0.8	1.2	29.1	9.2	8.0	-12.4
3c	1.1	0.9	0.9	28.2	9.8	6.4	-12.4
H ₃ B ₃ O ₃	0.2	-1.6	-1.6	18.9	-1.9	-1.9	-9.8

^aAll values are in ppm. ^bcc-pVTZ-PP on Sb, Bi, and Sn. ^cNICS values computed 1 Å away from the geometric center of the heteroboroxine ring on the same side (1) and opposite side (-1) as the pincer-type ligand L on the Sb or Bi. ^dNICS based on the out-of-plane zz shielding tensor component. ^eAverage of the in-plane components of the shielding tensor. ^fOn B3LYP/cc-pVTZ geometries.

Table 2. Relevant Bond Distances (*r*, Angstroms), Wiberg Bond Indices (WBI), and NPA Atomic Charges for Model Compounds 1, 2, and 3, Parent Boroxine H₃B₃O₃, and Extended Model Compounds 1', 2', and 3'

molecule	r _{B-O(M)}	r _{B-O(B)}	WBI _{B-O(M)}	WBI _{B-O(B)}	WBI _{M-O}	q _M	q _{O(M)}	q _{O(B)}	q _B
1	1.358	1.378	1.000	0.883	0.583	1.460	-1.009	-0.878	0.941
2	1.354	1.380	1.028	0.879	0.570	1.483	-1.000	-0.883	0.934
3	1.358	1.381	0.893	0.825	0.533	1.675	-1.018	-0.882	0.937
1'	1.355	1.387	1.004	0.862	0.465	1.674	-1.060	-0.890	1.104
2'	1.352	1.388	1.029	0.858	0.44	1.703	-1.062	-0.898	1.082
3'	1.354	1.389	1.015	0.859	0.421	2.090	-1.070	-0.896	1.088
H ₃ B ₃ O ₃			0.904	0.904			-0.856	-0.856	0.958

basically have the same energy (see Supporting Information). Thus, it seems that the orientation of the substituents is not determined by single-molecule effects but results from the crystal packing.

The redox properties of ferrocenylated derivatives 1c, 2c, and 3c were studied by cyclic voltammetry at the Pt disc electrode in 1,2-dichloroethane containing 0.1 M Bu₄N[PF₆] as the supporting electrolyte. Compounds showed only one wave attributable to the ferrocene/ferrocenium couple (Figure S1, Supporting Information). The redox change was controlled by diffusion as indicated by *i*_{pa} (anodic peak current) increasing linearly with the square root of the scan rate (*i*_{pa} ∝ ν^{1/2}). However, the observed waves were composite resulting from a convolution of two narrow-spaced one-electron redox waves (anodic peak potential, *E*_{pa} = 0.575 V for 1c, 0.540 V for 2c, and 0.550 V for 3c vs decamethylferrocene/decamethylferrocenium;¹⁸ peak separations were ca. 140 mV for 1c and 2c and 120 mV for 3c). The composite nature of the redox waves suggests a weak, probably electrostatic communication between the ferrocenyl substituents and was confirmed by square-wave voltammograms (Figure S2, Supporting Information). It is also noteworthy that the primary electrochemical reaction was not fully reversible, giving rise to another electrochemically active compound, which was reduced at a relatively lower potential (and also oxidized during the second or following scans; see Figure S1, Supporting Information).

The bonding situation in the heteroboroxines was studied theoretically using DFT computations. As a first step, the molecular structures of compounds 1a, 1c, 2b, 3b, and 3c were optimized from the crystal structure geometries at the

B3LYP¹⁹/cc-pVDZ²⁰ (cc-pVDZ-PP²¹ for Sb, Bi, and Sn) level of theory. The computed geometrical parameters were found to be in good agreement with the experimental values. The structures of 1b, 2a, 2c, and 3a were also constructed in silico and optimized at the same level of theory. Cartesian coordinates of all optimized geometries are given in the Supporting Information.

The observed shortening of the B–O bonds within all structurally characterized heteroboroxines 1a, 1c, 2b, 3b, and 3c may indicate a multiple character of these bonds. In order to investigate possible aromaticity of the heteroboroxines,²² the model compounds HSb[(OBH)₂O] (1), HBi[(OBH)₂O] (2), and H₂Sn[(OBH)₂O] (3) were constructed and optimized at the B3LYP¹⁹/cc-pVTZ²⁰ (cc-pVTZ-PP²¹ on Sb, Bi, or Sn) level. In all optimized model systems, confirmed to be minima on the potential energy surface by computation of the vibrational frequencies, the heteroboroxine ring is planar and the bond distances of the B–O(M) bonds are slightly shorter than the B–O(B) bonds, in agreement with experimental findings. The possible aromaticity of 1–3 through the magnetic criterion was assessed via computation of the different variations of the nucleus-independent chemical shifts (NICS)²³ and induced current densities.²⁴ These were compared with the properties of the parent boroxine H₃B₃O₃.²² Results are summarized in Table 1 together with results of the NICS evaluations in the real compounds 1a–c, 2a–c, and 3a–c. On the basis of the comparison of the NICS values in the center of the ring (NICS(0)), the NICS values 1 Å above and below the ring (NICS(±1)), and the component of the shielding tensor perpendicular to the ring plane component

of the shielding tensor, these rings can be classified as nonaromatic, in agreement with the parent boroxine.

This is nicely confirmed by current density plots (computed using the ipsocentric formalism;²⁴ see Figure S3, Supporting Information) showing only localized diatropic circulations around the oxygens and no diatropic or paratropic ring current, the footprint of an aromatic or nonaromatic ring. The bonding in the heteroboroxine rings was further investigated on the model compounds **1**, **2**, and **3** using natural bond orbitals²⁵ and Wiberg bond indices.²⁶ The Wiberg bond indices (Table 2) of the B–O(M) bonds are always higher than those of the B–O(B) bonds consistent with the shorter distance of the former as compared to the latter, which also well corresponds with the experimental results. The Wiberg bond index of the B–O bond in the parent boroxine H₃B₃O₃ is smaller than the bond order of the B–O(M) bonds for compounds **1** and **2**; in the case of compound **3**, these bond orders are comparable. The boroxine B–O bond order in H₃B₃O₃ is however larger than the B–O(B) bond orders in all compounds. For compounds **1** and **2**, NBO analysis reveals the presence of one largely s-type lone pair on Sb or Bi and two bonds from the metal atoms to the neighboring oxygen atoms (with bond orders of 0.583 and 0.570, respectively). In the case of compound **3**, four bonds emerge from the Sn atom to its neighbors with Wiberg bond indices of 0.533 (Sn–O) and 0.876 (Sn–H), respectively.

In order to investigate in more detail the presence of the pincer-type ligands on the heteroboroxine rings, larger model systems LSb[(OBMe)₂O] (**1'**), LBi[(OBMe)₂O] (**2'**), and L(Me)Sn[(OBMe)₂O] (**3'**) were constructed. These contain the ligands L on the metal atom, while methyl groups are used for termination of the free valencies. Relevant bond distances of the heteroboroxine rings remain essentially unaltered in these larger systems. In addition, NBO analysis is fully consistent with the bonding situation around the metal atoms in the simpler model systems **1–3**. The only differences are seen in the bond orders of the metal to oxygen bonds in the boroxine rings that are somewhat decreased (0.465 for **1'**, 0.440 for **2'**, and 0.421 for **3'**) and in the atomic charges on the metals that become more positive, favoring a stabilizing interaction with the negatively charged nitrogen atoms of the ligand L. Both facts reflect significant polarization of the M–O bonds in **1'–3'** in comparison with **1–3** induced by the pincer ligand.

CONCLUSION

We discovered a new straightforward and high-yielding synthetic route to novel heteroboroxines possessing Sb, Bi, and Sn heteroatoms in the central MB₂O₃ ring. Theoretical considerations proved nonaromatic character of these heteroboroxines and suggest that the presence of the pincer-type ligand leads to a significant polarization of the MB₂O₃ moieties. Results of further reactivity studies and attempts at preparation of other heteroboroxines bearing various substituents at boron and heteroatoms M will be reported in due course.

EXPERIMENTAL SECTION

General Remarks. ¹H, ¹¹B, ¹³C, and ¹¹⁹Sn NMR spectra were recorded on a Bruker Avance 500 MHz spectrometer or Bruker Ultrashield 400 MHz using a 5 mm tunable broad-band probe. Appropriate chemical shifts in ¹H and ¹³C NMR spectra were related to the residual signals of the solvent (CDCl₃: δ(¹H) = 7.27 ppm and δ(¹³C) = 77.23 ppm) or to the external Me₄Sn δ(¹¹⁹Sn) = 0.00 ppm in the case of the ¹¹⁹Sn NMR spectra. ¹¹B NMR spectra were related to external standard B(OMe)₃ (δ(¹⁰B) = 18.1 ppm). IR spectra were

recorded in the 4000–50 cm⁻¹ region on a Nicolet 6700 FTIR spectrometer using a single-bounce diamond ATR crystal. Elemental analyses were performed on an LECO-CHNS-932 analyzer. Starting compounds (LSbO)₂,^{14a} (LBiO)₂,^{14b} and L(Ph)Sn(CO₃)^{14c} were prepared according to literature procedures.

Syntheses. **Compound LSb[(OBPh)₂O] (**1a**).** A solution of (LSbO)₂ (417 mg, 0.63 mmol) in CH₂Cl₂ (20 mL) was added to a stirred solution of PhB(OH)₂ (309 mg, 2.53 mmol) in CH₂Cl₂ (15 mL) at room temperature, and the reaction mixture was stirred for an additional 12 h at this temperature. Then the volume of the solution was evaporated to ca. 5 mL; hexane (15 mL) was added leading to formation of a white precipitate. The white solid was collected by filtration, washed with 5 mL of hexane, and dried in vacuo to give **1a** as a white solid. Yield: 571 mg (84%). Mp: 155–157 °C. ¹H NMR (CDCl₃, 25 °C): δ = 2.19 (s(br), 6H, (CH₃)₂N), 2.84 (s(br), 6H, (CH₃)₂N), 3.09 and 4.75 (AX pattern, 4H, CH₂N), 7.03 (d, 2H, L-Ph-H3,5), 7.17 (t, 1H, L-Ph-H4), 7.38 (m, 6H, B-Ph3,4,5), 8.02 (d, 4H, B-Ph2,6). ¹³C{¹H} NMR (CDCl₃, 25 °C): δ = 42.4 ((CH₃)₂N), 45.0 ((CH₃)₂N), 63.3 (CH₂N), 126.3 (L-Ph-C3,5), 127.6 (B-Ph-C3,5), 129.3 (L-Ph-C4), 130.1 (B-Ph-C4), 135.0 (B-Ph-C2,6), 147.4 (L-Ph-C2,6), 155.5 (L-Ph-C1). ¹¹B{¹H} NMR (CDCl₃, 25 °C): δ = 26.9. Anal. Calcd for C₂₄H₂₉N₂O₃B₂Sb (536.86): C, 53.7; H, 5.4. Found: C, 54.0; H, 5.1.

Compound LSb[(OB-4-CF₃C₆H₄)₂O] (1b**).** A solution of (LSbO)₂ (205 mg, 0.31 mmol) in CH₂Cl₂ (20 mL) was added to a stirred suspension of 4-CF₃C₆H₄B(OH)₂ (237 mg, 1.25 mmol) in CH₂Cl₂ (15 mL) at room temperature, and the reaction mixture was stirred for additional 12 h at this temperature whereupon a clear solution resulted. Then the volume of the solution was evaporated to ca. 5 mL; hexane (15 mL) was added, leading to formation of a white precipitate. The white solid was collected by filtration, washed with 5 mL of hexane, and dried in vacuo to give **1b** as a white solid. Yield: 334 mg (80%). Mp: 199–202 °C. ¹H NMR (CDCl₃, 25 °C): δ = 2.10 (s(br), 6H, (CH₃)₂N), 2.86 (s(br), 6H, (CH₃)₂N), 3.12 and 4.68 (AX pattern, 4H, CH₂N), 7.06 (d, 2H, L-Ph-H3,5), 7.21 (t, 1H, L-Ph-H4), 7.63 (d, 4H, B-Ph3,5), 8.08 (d, 4H, B-Ph2,6). ¹³C{¹H} NMR (CDCl₃, 25 °C): δ = 42.4 ((CH₃)₂N), 45.5 ((CH₃)₂N), 63.2 (CH₂N), 124.2 (q, B-Ph-C3,5, ³J(C,F) = 4 Hz), 126.3 (q, CF₃, ¹J(C,F) = 265 Hz), 126.4 (L-Ph-C3,5), 129.6 (L-Ph-C4), 131.7 (q, B-Ph-C4, ²J(C,F) = 32 Hz), 135.0 (B-Ph-C2,6), 141.4 (B-Ph-C1), 147.2 (L-Ph-C2,6), 155.1 (L-Ph-C1). ¹¹B{¹H} NMR (CDCl₃, 25 °C): δ = 27.5. ¹⁹F NMR (CDCl₃, 25 °C): δ = -62.6. Anal. Calcd for C₂₆H₂₇N₂O₃F₆B₂Sb: C, 46.2; H, 4.7. Found: C, 46.5; H, 4.4.

Compound LSb[(OBFc)₂O] (1c**).** A solution of (LSbO)₂ (98 mg, 0.15 mmol) in CH₂Cl₂ (20 mL) was added to a stirred solution of FcB(OH)₂ (138 mg, 0.60 mmol) in CH₂Cl₂ (15 mL) at room temperature, and the reaction mixture was stirred for an additional 12 h at this temperature. Then the volume of the solution was evaporated to ca. 5 mL; hexane (15 mL) was added, leading to formation of a yellow-orange precipitate. Solid was collected by filtration, washed with 5 mL of hexane, and dried in vacuo to give **1c** as a yellow solid. Yield: 172 mg (84%). Mp >250 °C. ¹H NMR (CDCl₃, 25 °C): δ = 2.15 (s(br), 6H, (CH₃)₂N), 2.80 (s(br), 6H, (CH₃)₂N), 3.15 and 4.89 (AX pattern, 4H, CH₂N), 3.96 (s, 10H CpFe), 4.33 (s, 4H, Cp(BO₂)Fe), 4.42 (s, 2H, Cp(BO₂)Fe), 4.50 (2H, s, Cp(BO₂)Fe), 7.10 (d, 2H, L-Ph-H3,5), 7.16 (t, 1H, L-Ph-H4). ¹³C{¹H} NMR (CDCl₃, 25 °C): δ = 42.5 ((CH₃)₂N), 44.9 ((CH₃)₂N), 63.4 (CH₂N), 68.3 (CpFe), 71.2 (Cp(BO₂)Fe), 71.3 (Cp(BO₂)Fe), 73.8 (Cp(BO₂)Fe), 74.5 (Cp(BO₂)Fe), 126.5 (L-Ph-C3,5), 129.5 (L-Ph-C4), 147.3 (L-Ph-C2,6), 155.9 (L-Ph-C1). ¹¹B{¹H} NMR (CDCl₃, 25 °C): δ = 29.3. Anal. Calcd for C₃₂H₃₇N₂O₃Fe₂B₂Sb: C, 51.0; H, 4.9. Found: C, 51.3; H, 4.7.

Compound LBi[(OBPh)₂O] (2a**).** A solution of (LBiO)₂ (189 mg, 0.23 mmol) in toluene (20 mL) was added to a stirred solution of PhB(OH)₂ (111 mg, 0.91 mmol) in toluene (20 mL) at room temperature, and the reaction mixture was stirred for an additional 12 h at this temperature. Then the volume of the resulting solution was evaporated to ca. 5 mL; hexane (10 mL) was added, causing a separation of a white precipitate. White solid was collected by filtration, washed with 5 mL of hexane, and dried in vacuo to give **2a** as

Table 3. Crystallographic Data for 1a, 1c, 2b, 3b, and 3c

	1a	1c	2b	3b	3c
chemical formula	C ₂₄ H ₂₉ B ₂ N ₂ O ₃ Sb	C ₃₂ H ₃₇ B ₂ N ₂ Fe ₂ O ₃ Sb	C ₂₆ H ₂₇ B ₂ BiF ₆ N ₂ O ₃	C ₃₂ H ₃₂ B ₂ F ₆ N ₂ O ₃ Sn	C ₃₈ H ₄₂ B ₂ Fe ₂ N ₂ O ₃ Sn
cryst syst	monoclinic	monoclinic	orthorhombic	monoclinic	orthorhombic
space group	<i>P</i> 2 ₁ / <i>c</i>	<i>P</i> 2 ₁ / <i>c</i>	<i>Pnma</i>	<i>P</i> 2 ₁ / <i>c</i>	<i>P</i> 2 ₁ 2 ₁
<i>a</i> [Å]	6.5320(5)	20.4090(9)	12.6610(9)	22.3600(6)	11.5029(13)
<i>b</i> [Å]	31.944(3)	12.1311(10)	24.1351(10)	13.2700(10)	16.3892(14)
<i>c</i> [Å]	12.5390(3)	12.4800(14)	9.2950(13)	11.0911(16)	18.9900(13)
α [deg]	90	90	90	90	90
β [deg]	113.171(5)	95.455(5)	90	93.940(6)	90
γ [deg]	90	90	90	90	90
<i>Z</i>	4	4	4	4	4
μ [mm ⁻¹]	1.175	1.839	6.277	0.848	1.531
<i>D_x</i> [Mg m ⁻³]	1.483	1.625	1.778	1.511	1.534
cryst size [mm]	0.33 × 0.16 × 0.12	0.37 × 0.09 × 0.07	0.26 × 0.17 × 0.10	0.34 × 0.25 × 0.04	0.47 × 0.29 × 0.20
θ range [deg]	1–27.5	1–27.5	1–27.5	1–27.5	1–27.5
<i>T</i> _{min} / <i>T</i> _{max}	0.835, 0.891	0.779, 0.891	0.425, 0.691	0.864, 0.964	0.636, 0.791
no. of reflns measd	23 671	26 518	20 374	29 517	25 341
no. of unique reflns, <i>R</i> _{int} ^a	5415, 0.039	7004, 0.055	3325, 0.040	7497, 0.066	8054, 0.041
no. of obsd reflns [<i>I</i> > 2 σ (<i>I</i>)]	4339	5357	2729	5245	7293
no. of params	289	379	187	415	433
<i>S</i> ^b all data	1.087	1.100	1.098	1.117	1.130
final <i>R</i> ^c indices [<i>I</i> > 2 σ (<i>I</i>)]	0.033	0.039	0.040	0.058	0.032
w <i>R</i> ² indices (all data)	0.058	0.062	0.085	0.105	0.058
$\Delta\rho$, max, min [e Å ⁻³]	0.391, -0.577	0.512, -0.661	1.792, -1.162	1.902, -0.890	0.573, -0.547

^a*R*_{int} = $\sum(F_o^2 - F_c^2)/\sum F_o^2$. ^b*S* = $[\sum(w(F_o^2 - F_c^2)^2)/(N_{\text{diffs}} - N_{\text{params}})]^{1/2}$. ^c*R*(*F*) = $\sum|F_o| - |F_c|/\sum|F_o|$, w*R*(*F*²) = $[\sum(w(F_o^2 - F_c^2)^2)/(\sum w(F_o^2)^2)]^{1/2}$.

a white solid. Yield: 219 mg (95%). Mp: 170–174 °C. ¹H NMR (CDCl₃, 25 °C): δ = 2.17 (s(br), 6H, (CH₃)₂N), 2.93 (s(br), 6H, (CH₃)₂N), 3.29 and 4.76 (AX pattern, 4H, CH₂N), 7.25 (t, 1H, L-Ph-H4), 7.39 (m, 8H, L-Ph-H3,5 and B-Ph3,4,5), 8.04 (d, 4H, B-Ph2,6). ¹³C{¹H} NMR (CDCl₃, 25 °C): δ = 42.5 ((CH₃)₂N), 46.2 ((CH₃)₂N), 65.7 (CH₂N), 127.6 (B-Ph-C3,5), 128.5 (L-Ph-C3,5), 128.7 (L-Ph-C4), 129.6 (B-Ph-C4), 135.1 (B-Ph-C2,6), 152.1 (L-Ph-C2,6), 205.0 (L-Ph-C1). ¹¹B{¹H} NMR (CDCl₃, 25 °C): δ = 26.7. Anal. Calcd for C₂₄H₂₉N₂O₃B₂Bi: C, 46.2; H, 4.7. Found: C, 46.3; H, 4.6.

Compound LBi[(OB-4-CF₃C₆H₄)₂O] (2b). A solution of (LBiO)₂ (100 mg, 0.12 mmol) in toluene (20 mL) was added to a stirred suspension of 4-CF₃C₆H₄B(OH)₂ (91 mg, 0.48 mmol) in the same solvent (15 mL) at room temperature. The reaction mixture was stirred for an additional 12 h at this temperature, affording a clear solution. Then the volume of the solution was evaporated to ca. 5 mL; hexane (15 mL) was added, leading to formation of a white precipitate. White solid was collected by filtration, washed with 5 mL of hexane, and dried in vacuo to give 2b as a white solid. Yield: 182 mg (90%). Mp: 184–187 °C. ¹H NMR (400 MHz, CDCl₃, 25 °C): δ = 2.17 (s(br), 6H, (CH₃)₂N), 2.93 (s(br), 6H, (CH₃)₂N), 3.35 and 4.70 (AX pattern, 4H, CH₂N), 7.29 (t, 1H, L-Ph-H4), 7.42 (d, 2H, L-Ph-H3,5), 7.61 (d, 4H, B-Ph3,5), 8.08 (d, 4H, B-Ph2,6). ¹³C{¹H} NMR (100.6 MHz, CDCl₃, 25 °C): δ = 42.5 ((CH₃)₂N), 46.3 ((CH₃)₂N), 65.7 (CH₂N), 124.2 (q, B-Ph-C3,5, ³J(C,F) = 4 Hz), 124.2 (q, CF₃, ¹J(C,F) = 266 Hz), 128.7 (L-Ph-C3,5), 129.1 (L-Ph-C4), 131.3 (q, B-Ph-C4, ²J(C,F) = 32 Hz), 135.3 (B-Ph-C2,6), 138.1 (B-Ph-C1), 152.2 (L-Ph-C2,6), 205.4 (L-Ph-C1). ¹¹B{¹H} NMR (CDCl₃, 25 °C): δ = 26.4. ¹⁹F NMR (CDCl₃, 25 °C): δ = -62.6. Anal. Calcd for C₂₆H₂₇N₂O₃F₆B₂Bi: C, 41.1; H, 3.6. Found: C, 41.4; H, 3.4.

Compound LBi[(OBFC)₂O] (2c). A solution of (LBiO)₂ (100 mg, 0.12 mmol) in toluene (20 mL) was added to a stirred solution of FcB(OH)₂ (110 mg, 0.48 mmol) in toluene (15 mL) at room temperature. The reaction mixture was stirred for an additional 12 h at this temperature. Then the volume of the solution was evaporated to ca. 5 mL; hexane (15 mL) was added, leading to formation of a yellow-orange precipitate. Solid was collected by filtration, washed with 5 mL of hexane, and dried in vacuo to give compound 2c as a yellow solid.

Yield: 156 mg (86%). Mp: >237 °C (dec). ¹H NMR (CDCl₃, 25 °C): δ = 2.18 (s(br), 6H, (CH₃)₂N), 2.67 (s(br), 6H, (CH₃)₂N), 3.35 and 4.93 (AX pattern, 4H, CH₂N), 3.95 (s, 10H CpFe), 4.30 (s, 4H, Cp(BO₂)Fe), 4.40 (s, 2H, Cp(BO₂)Fe), 4.91 (2H, s, Cp(BO₂)Fe), 7.26 (t, 1H, L-Ph-H4), 7.47 (d, 2H, L-Ph-H3,5). ¹³C{¹H} NMR (CDCl₃, 25 °C): δ = 42.0 ((CH₃)₂N), 45.7 ((CH₃)₂N), 65.7 (CH₂N), 68.2 (CpFe), 71.0 (Cp(BO₂)Fe), 73.6 (Cp(BO₂)Fe), 74.7 (Cp(BO₂)Fe), 128.6 (L-Ph-C3,5), 128.9 (L-Ph-C4), 152.0 (L-Ph-C2,6), (L-Ph-C1) not found. ¹¹B{¹H} NMR (CDCl₃, 25 °C): δ = 28.4. Anal. Calcd for C₃₂H₃₇N₂O₃Fe₂B₂Bi: C, 45.6; H, 4.4. Found: C, 45.9; H, 4.1.

Compound LSn(Ph)[(OBPh)₂O] (3a). PhB(OH)₂ (77.8 mg; 0.64 mmol) was added to a stirred solution of L(Ph)Sn(CO₃) (142.6 mg; 0.32 mmol) in CH₂Cl₂ (20 mL) at room temperature. The reaction mixture was stirred for an additional 24 h and then evaporated. White solid residue was washed with hexane (5 mL) and dried in vacuo to give 3a as a white solid. Yield: 571 mg (84%). Mp: 119–124 °C. ¹H NMR (CDCl₃, 25 °C): δ = 2.31 (s, 12H, (CH₃)₂N), 3.10 and 4.70 (AX pattern, 4H, CH₂N), 7.15 (d, 2H, ArH), 7.31 (t, 1H, ArH), 7.49 (m, 9H, ArH), 7.82 (d, 2H, ArH), 8.20 (d, 4H, ArH). ¹³C{¹H} NMR (CDCl₃, 25 °C): δ = 44.8 ((CH₃)₂N), 63.1 (CH₂N), 127.2 (Ph-C3,5), 127.4 (B-Ph-C3,5), 128.1 (L-Ph-C3,5), 129.6 (Ph-C4), 129.7 (B-Ph-C4), 130.1 (L-Ph-C4), 134.6 (Ph-C2,6), 134.9 (B-Ph-C2,6), 138.3 (B-Ph-C1), 139.3 (Ph-C1), 141.9 (L-Ph-C1), 145.2 (L-Ph-C2,6). ¹¹B{¹H} NMR (CDCl₃, 25 °C): δ = 27.1. ¹¹⁹Sn NMR (CDCl₃, 25 °C): δ = -359.1. Anal. Calcd for C₂₉H₃₂N₂O₃B₂Sn (476.76): C, 58.9; H, 5.6. Found: C, 58.5; H, 5.3.

Compound LSn(Ph)[(OB-4-CF₃C₆H₄)₂O] (3b). 4-CF₃C₆H₄-B(OH)₂ (122.6 mg; 0.32 mmol) was added to a stirred solution of L(Ph)Sn(CO₃) (144.3 mg; 0.65 mmol) in CH₂Cl₂ (20 mL) at room temperature. This reaction mixture was stirred for an additional 24 h at this temperature and then evaporated in vacuo. The resulting white solid was washed with hexane (5 mL) and dried in vacuo to give 3b as a white solid. Yield: 571 mg (84%). Mp: 189–191 °C. ¹H NMR (CDCl₃, 25 °C): δ = 2.48 (s, 12H, (CH₃)₂N), 3.19 and 4.71 (AX pattern, 4H, CH₂N), 7.23 (d, 2H, ArH), 7.43 (t, 1H, ArH), 7.56 (m, 1H, ArH), 7.78 (d, 6H, ArH), 7.85 (d, 2H, ArH), 8.29 (d, 4H, ArH). ¹³C{¹H} NMR (CDCl₃, 25 °C): δ = 44.7 ((CH₃)₂N), 63.1 (CH₂N), 123.3 (CF₃), 124.1 (B-Ph-C3,5), 126.1 (CF₃), 127.4 (Ph-C3,5), 128.8 (L-Ph-C3,5),

129.8 (L-Ph-C4), 130.4 (Ph-C4), 131.2 (B-Ph-C4), 131.5 (B-Ph-C4), 134.5 (Ph-C2,6), 135.0 (B-Ph-C2,6), 139.0 (Ph-C1), 141.4 (L-Ph-C1), 142.2 (B-Ph-C1), 145.0 (L-Ph-C2,6). $^{11}\text{B}\{^1\text{H}\}$ NMR (CDCl_3 , 25 °C): $\delta = 29.3$. ^{19}F NMR (CDCl_3 , 25 °C): $\delta = -62.5$. ^{119}Sn NMR (CDCl_3 , 25 °C): $\delta = -364.0$. Anal. Calcd for $\text{C}_{31}\text{H}_{36}\text{N}_2\text{O}_3\text{F}_6\text{B}_2\text{Sn}$ (490.77): C, 51.4; H, 4.3. Found: C, 51.1; H, 4.1.

Compound $\text{LSn(Ph)[(OBfC}_2\text{O)] (3c)$. FcB(OH)_2 (78.4 mg; 0.34 mmol) was added to a stirred solution of $\text{L(Ph)Sn(CO}_3\text{)}$ (76.2 mg; 0.17 mmol) in CH_2Cl_2 (20 mL) at room temperature, and the reaction mixture was stirred for a further 24 h at this temperature and evaporated in vacuo. The resulting orange solid was washed with hexane (5 mL) and dried in vacuo to give **3c** as an orange solid. Yield: 156 mg (86%). Mp: 213–215 °C. ^1H NMR (CDCl_3 , 25 °C): $\delta = 2.37$ (s, 12H, $(\text{CH}_3)_2\text{N}$), 3.11 and 4.73 (AX pattern, 4H, CH_2N), 4.05 (s, 10H CpFe), 4.35 (s, 4H, Cp(BO_2)Fe), 4.53 (s, 4H, Cp(BO_2)Fe), 7.14 (t, 2H, ArH), 7.31 (d, 1H, ArH), 7.14 (t, 3H, ArH), 7.85 (d, 2H, ArH). $^{13}\text{C}\{^1\text{H}\}$ NMR (CDCl_3 , 25 °C): $\delta = 44.7$ ($(\text{CH}_3)_2\text{N}$), 63.3 (CH_2N), 68.3 (CpFe), 71.1 (Cp(BO_2)Fe), 74.2 (Cp(BO_2)Fe), 127.3 (L-Ph-C3,5), 128.7 (Ph-C3,5), 129.7 (Ph-C4), 130.3 (L-Ph-C4), 134.9 (Ph-C2,6), 139.7 (Ph-C1), 142.2 (L-Ph-C1), 145.3 (L-Ph-C2,6). $^{11}\text{B}\{^1\text{H}\}$ NMR (CDCl_3 , 25 °C): $\delta = 28.2$. ^{119}Sn NMR (CDCl_3 , 25 °C): $\delta = -358.0$. Anal. Calcd for $\text{C}_{37}\text{H}_{42}\text{N}_2\text{O}_3\text{Fe}_2\text{B}_2\text{Sn}$: C, 45.6; H, 4.4. Found: C, 45.9; H, 4.1.

X-ray Diffraction Analyses. Suitable single crystals of **1a**, **1c**, **2b**, **3b**, and **3c** were mounted on a glass fiber with an oil and measured on a four-circle diffractometer KappaCCD with CCD area detector by monochromatized Mo $K\alpha$ radiation ($\lambda = 0.71073$ Å). Corresponding crystallographic data are given in Table 3. The numerical²⁷ absorption correction from the crystal shape was applied for all crystals. Structures were solved by direct methods (SIR92²⁸) and refined by a full matrix least-squares procedure based on F^2 (SHELXL97²⁹). Hydrogen atoms were mostly localized on a difference Fourier map; however, to ensure the uniformity of treatment of the crystal, all hydrogen were recalculated into idealized positions (riding model) and assigned temperature factors $H_{\text{iso}}(\text{H}) = 1.2U_{\text{eq}}(\text{pivot atom})$ or $1.5U_{\text{eq}}$ for the methyl moiety with C–H = 0.96, 0.98, and 0.93 Å for methyl, methylene, and hydrogen atoms in the aromatic rings, respectively. The final difference maps displayed no peaks of chemical significance as the highest peaks and holes are in close vicinity of heavy atoms. Crystallographic data for structural analysis has been deposited with the Cambridge Crystallographic Data Centre, CCDC nos. 895166–895170. Copies of this information may be obtained free of charge from The Director, CCDC, 12 Union Road, Cambridge CB2 1EY, UK (Fax +44-1223-336033; e-mail deposit@ccdc.cam.ac.uk or http://www.ccdc.cam.ac.uk).

Computational Details. Model compounds **1**, **2**, and **3**, the parent boroxine $\text{H}_3\text{B}_3\text{O}_3$, and the “extended” model compounds **1'**, **2'**, and **3'** were optimized at the B3LYP level of theory¹⁹ using the cc-pVTZ basis set²⁰ (cc-pVTZ-PP²¹ basis set for Sb, Bi, and Sn). Subsequent NBO analysis²⁵ and calculation of Wiberg bond indices²⁶ and nucleus-independent chemical shifts²³ (for **1**, **2**, and **3**) were performed at the same level of theory. In addition, the current density induced by the external magnetic field, directed perpendicular to the ring of interest, was calculated for **1**, **2**, and **3** at the same level of theory using the ipsocentric CTOCD-DZ method.²⁴ Compounds **1a–c**, **2a–c**, and **3a–c** were optimized at the B3LYP level of theory¹⁸ using the cc-pVDZ basis set (cc-pVDZ-PP basis set for Sb, Bi, and Sn). Subsequent NBO analysis²¹ and calculation of Wiberg bond indices²⁵ and nucleus-independent chemical shifts²⁶ for these compounds were performed at the same level of theory. All calculations were performed using the Gaussian 09 program,³⁰ except for computation of the induced current densities, which were performed using the GAMESS-UK³¹ and SYSMO programs.³²

■ ASSOCIATED CONTENT

Supporting Information

Figures S1–S3, crystallographic data in cif format, and details of DFT calculations together with ball and stick representation and Cartesian coordinates (Å) of optimized compounds. This

material is available free of charge via the Internet at <http://pubs.acs.org>.

■ AUTHOR INFORMATION

Corresponding Author

*E-mail: fdeprof@vub.ac.be (F.D.P.); roman.jambor@upce.cz (R.J.); libor.dostal@upce.cz (L.D.).

Notes

The authors declare no competing financial interest.

■ ACKNOWLEDGMENTS

This work was financially supported by the Czech Science Foundation (project no. P207/13-00289S), the Fund for Scientific Research Flanders (Belgium) FWO, the Vrije Universiteit Brussel, the Zernike Institute for Advanced Materials (“Dieptestrategie” program), and the Ministry of Education, Youth and Sports of the Czech Republic (project no. MSM0021620857).

■ DEDICATION

Dedicated to Prof. Jaroslav Holeček on the occasion of his 80th birthday.

■ REFERENCES

- Hall, D. G.; Frye, G. C. In *Boronic Acids*; Wiley-VCH: Weinheim, 2005.
- (a) Korich, A. L.; Iovine, P. M. *Dalton. Trans.* **2010**, 39, 1423. (b) Westcott, S. A. *Angew. Chem., Int. Ed.* **2010**, 49, 9045.
- Cote, A. P.; Benin, A. I.; Ockwig, N. W.; O’Keeffe, M.; Matzger, A. J.; Yaghi, O. M. *Science* **2005**, 310, 1166.
- (a) Cambell, N. L.; Clowes, R.; Ritchie, L. K.; Cooper, A. I. *Chem. Mater.* **2009**, 21, 204. (b) Cao, D.; Lan, J.; Wang, W.; Smith, B. *Angew. Chem., Int. Ed.* **2009**, 48, 4730. (c) El-Kaderi, H. M.; Hunt, J. R.; Mendoza-Cortes, J. L.; Cote, A. P.; Taylor, R. E.; O’Keeffe, M.; Yaghi, M. *Science* **2007**, 316, 268. (d) Han, S. S.; Furukava, H.; Yaghi, O. M.; Goddard, W. A. *J. Am. Chem. Soc.* **2008**, 130, 11580. (e) Tilford, R. W.; Gemmill, W. R.; zur Loye, H.-C.; Lavigne, J. J. *Chem. Mater.* **2008**, 20, 2741. (f) Mastalerz, M. *Angew. Chem., Int. Ed.* **2008**, 120, 445.
- (a) Forsyth, M.; Sun, J.; Zhou, F.; MacFarlane, D. R. *Electrochim. Acta* **2003**, 48, 2129. (b) Mehta, M. A.; Fujinami, T.; Inoue, S.; Matsushita, K.; Miwa, T.; Inoue, T. *Electrochim. Acta* **2000**, 45, 1175. (c) Nair, N. G.; Blanco, M.; West, W.; Weisse, F. C.; Greenbaum, S.; Reddy, V. P. *J. Phys. Chem. A* **2009**, 113, 5918. (d) Yang, Y.; Inoue, T.; Fujinami, T.; Mehta, M. A. *J. Appl. Polym. Sci.* **2002**, 84, 17.
- (a) Alcaraz, G.; Euzenat, L.; Mongin, O.; Katan, C.; Ledoux, I.; Zyss, J.; Blanchard-Desce, M.; Vaultier, M. *Chem. Commun.* **2003**, 2766. (b) Oliva, M. M.; Casado, J.; Hennrich, G.; Navarrete, J. T. L. *J. Phys. Chem. B* **2006**, 110, 19198.
- For recent example see: (a) Graham, T. J. A.; Shields, J. D.; Doyle, A. G. *Chem. Sci.* **2011**, 2, 980. (b) Xu, L.; Li, B. J.; Wu, Z. H.; Lu, X. Y.; Guan, B. T.; Wang, B. Q.; Zhao, K. Q.; Shi, Z. J. *Org. Lett.* **2010**, 12, 884. (c) Song, Z. Z.; Wong, H. N. C.; Yang, Y. *Pure Appl. Chem.* **1996**, 68, 723.
- (a) Beckmann, J.; Dakternieks, D.; Duthie, A.; Lim, A. E. K.; Tiekink, E. R. T. *J. Organomet. Chem.* **2001**, 633, 149. (b) Zhu, L.; Shabbir, S. H.; Gray, M.; Lynch, V. M.; Sorey, S.; Anslyn, E. V. *J. Am. Chem. Soc.* **2006**, 128, 1222. (c) Synder, R. H.; Konecky, M. S.; Lennarz, W. J. *J. Am. Chem. Soc.* **1958**, 80, 3611. (d) Norrild, J. C.; Sotofte, I. *J. Chem. Soc., Perkin Trans. 2* **2002**, 303. (e) Das, M. K.; Mariategui, J. F.; Neidenzu, K. *Inorg. Chem.* **1987**, 26, 3114.
- (a) Thilagar, P.; Chen, J.; Lalancette, R. A.; Jäkle, F. *Organometallics* **2011**, 30, 6734. (b) Park, K.-S.; Schougaard, S. B.; Goodenough, J. B. *Adv. Mater.* **2007**, 19, 848. (c) Tamura, K.; Akutagawa, N.; Satoh, M.; Wada, J.; Masuda, T. *Macromol. Rapid Commun.* **2008**, 29, 1944. (d) Bats, J. W.; Ma, K.; Wagner, M. *Acta Crystallogr. C* **2002**, C58, m129. (e) Braunschweig, H.; Bera, H.;

- Stellwag, S.; Schwarz, S.; Hemberger, Y.; Radacki, K. Z. *Anorg. Allg. Chem.* **2007**, *633*, 2314. (f) Chen, T. H.; Kaveevivitchai, W.; Bui, N.; Miljanić, O. *Chem. Commun.* **2012**, *48*, 2855.
- (10) (a) Ma, X.; Yang, Z.; Wang, X.; Roesky, H. W.; Wu, F.; Zhu, H. *Inorg. Chem.* **2011**, *50*, 2010. (b) Yang, Z.; Ma, X.; Oswald, R. B.; Roesky, H. W.; Noltemeyer, M. *J. Am. Chem. Soc.* **2006**, *128*, 12406.
- (11) (a) Liu, W. J.; Pink, M.; Lee, D. *J. Am. Chem. Soc.* **2009**, *131*, 8703. (b) Avent, A. G.; Lawrence, S. E.; Meehan, M. M.; Russell, T. G.; Spalding, T. R. *Collect. Czech. Chem. Commun.* **2002**, *67*, 1051.
- (12) Brown, P.; Mahon, M. F.; Molloy, K. C. *Dalton Trans.* **1992**, 3503.
- (13) Vargas, G.; Hernández, I.; Höpfl, H.; Ochoa, M. E.; Castillo, D.; Farfán, N.; Santillan, R.; Gómez, E. *Inorg. Chem.* **2004**, *43*, 8490.
- (14) (a) Dostál, L.; Jambor, R.; Růžička, A.; Erben, M.; Jirásko, R.; Černošková, Z.; Holeček, J. *Organometallics* **2009**, *28*, 2633. (b) Fridrichová, A.; Svoboda, T.; Jambor, R.; Padělková, Z.; Růžička, A.; Erben, M.; Jirásko, R.; Dostál, L. *Organometallics* **2009**, *28*, 5522. (c) Mayrichová, B.; Dostál, L.; Růžička, A.; Beneš, L.; Jambor, R. *J. Organomet. Chem.* **2012**, *699*, 1. (d) Svoboda, T.; Jambor, R.; Růžička, A.; Padělková, Z.; Erben, M.; Jirásko, R.; Dostál, L. *Eur. J. Inorg. Chem.* **2010**, 1663. (e) Svoboda, T.; Jambor, R.; Růžička, A.; Padělková, Z.; Erben, M.; Dostál, L. *Eur. J. Inorg. Chem.* **2010**, 5222. (f) Svoboda, T.; Dostál, L.; Jambor, R.; Růžička, A.; Jirásko, R.; Lyčka, A. *Inorg. Chem.* **2011**, *50*, 6411. (g) Svoboda, T.; Jambor, R.; Růžička, A.; Jirásko, R.; Lyčka, A.; de Proft, F.; Dostál, L. *Organometallics* **2012**, *31*, 1725.
- (15) (a) Pyykkö, P.; Atsumi, M. *Chem.—Eur. J.* **2009**, *15*, 186. (b) Pyykkö, P.; Atsumi, M. *Chem.—Eur. J.* **2009**, *15*, 12770. (c) Pyykkö, P.; Riedel, S.; Patzschke, M. *Chem.—Eur. J.* **2005**, *11*, 3511.
- (16) (a) Kašná, B.; Jambor, R.; Dostál, L.; Kolářová, L.; Císařová, I.; Holeček, J. *Organometallics* **2006**, *25*, 148. (b) Kašná, B.; Jambor, R.; Dostál, L.; Růžička, A.; Císařová, I.; Holeček, J. *Organometallics* **2004**, *23*, 5300. (c) Jambor, R.; Dostál, L.; Růžička, A.; Císařová, I.; Brus, J.; Holčapek, M.; Holeček, J. *Organometallics* **2002**, *21*, 3996.
- (17) Boese, R.; Polk, M.; Blaser, D. *Angew. Chem., Int. Ed.* **1987**, *26*, 245.
- (18) The redox potentials in the conventional ferrocene/ferrocenium scale would be ca. 0.025 (1c), -0.010 (2c), and 0 V (3c). These values were calculated using the difference in the redox potentials of the Fe(II/III) couple of ferrocene and decamethylferrocene obtained in dichloromethane: Barriere, F.; Geiger, W. E. *J. Am. Chem. Soc.* **2006**, *128*, 3980.
- (19) (a) Becke, A. D. *J. Chem. Phys.* **1993**, *98*, 5648. (b) Lee, C.; Yang, W.; Parr, R. G. *Phys. Rev. B* **1988**, *37*, 785. (c) Stephens, P. J.; Devlin, F. J.; Chabalowski, C. F.; Frisch, M. J. *J. Phys. Chem.* **1994**, *98*, 11623.
- (20) (a) Hydrogen and first row: Dunning, T. H. *J. Chem. Phys.* **1989**, *90*, 1007. (b) Second row: Woon, D. E.; Dunning, T. H. *J. Chem. Phys.* **1993**, *98*, 1358.
- (21) Peterson, K. A. *J. Chem. Phys.* **2003**, *119*, 11099.
- (22) For similar studies dealing with classical boroxines, see: (a) Archibong, E. F.; Thakkar, A. *J. Mol. Phys.* **1994**, *81*, 557. (b) Fowler, P. W.; Steiner, E. *J. Phys. Chem. A* **1997**, *101*, 1409. (c) Schleyer, P. v. R.; Jiao, H.; van Eikema Hommes, N. J. R.; Malkin, V. G.; Malkina, O. *J. Am. Chem. Soc.* **1997**, *119*, 12669. (d) Lamb, D. W.; Kier, R. I.; Ritchie, G. D. L. *Chem. Phys. Lett.* **1998**, *291*, 197.
- (23) (a) Schleyer, P. v. R.; Maerker, C.; Dransfeld, A.; Jiao, H.; van Eikema Hommes, N. *J. Am. Chem. Soc.* **1996**, *118*, 6317. (b) For a review, see e.g. Chen, Z.; Wannere, C. S.; Corminboeuf, C.; Puchta, R.; Schleyer, P. v. R. *Chem. Rev.* **2005**, *105*, 3842. (c) Fallah-Bagher-Shadaei, H.; Wannere, C. S.; Corminboeuf, C.; Puchta, R.; Schleyer, P. v. R. *Org. Lett.* **2006**, *8*, 863.
- (24) (a) Keith, T.; Bader, R. F. W. *Chem. Phys. Lett.* **1993**, *210*, 223. (b) Lazzarretti, P.; Malagoli, M.; Zanasi, R. *Chem. Phys. Lett.* **1994**, *220*, 299. (c) Steiner, E.; Fowler, P. W. *J. Phys. Chem. A* **2001**, *105*, 9553.
- (25) (a) Foster, J. P.; Weinhold, F. *J. Am. Chem. Soc.* **1980**, *102*, 7211. (b) Reed, A. E.; Weinhold, F. *J. Chem. Phys.* **1983**, *78*, 4066. (c) Reed, A. E.; Weinstock, R. B.; Weinhold, F. *J. Chem. Phys.* **1985**, *83*, 735. (d) Reed, A. E.; Curtiss, L. A.; Weinhold, F. *Chem. Rev.* **1988**, *88*, 899.
- (e) Weinhold, F. In *Encyclopedia of Computational Chemistry*; Schleyer, P. v. R., Allinger, N. L., Clark, T., Gasteiger, J., Kollman, P. A., Schaefer III, H. F., Schreiner, P. R., Eds.; John Wiley & Sons: Chichester, UK, 1998; Vol. 3 p 1792.
- (26) Wiberg, K. B. *Tetrahedron* **1968**, *24*, 1083.
- (27) Coppens, P. In *Crystallographic Computing*; Ahmed, F. R., Hall, S. R., Huber, C. P., Eds.; Munksgaard: Copenhagen, 1970; p 255.
- (28) Altomare, A.; Casciarone, G.; Giacovazzo, C.; Guagliardi, A.; Burla, M. C.; Polidori, G.; Camalli, M. *J. Appl. Crystallogr.* **1994**, *27*, 1045.
- (29) Sheldrick, G. M. *SHELXL-97, A Program for Crystal Structure Refinement*; University of Göttingen: Germany, 1997.
- (30) Frisch, M. J.; Trucks, G. W.; Schlegel, H. B.; Scuseria, G. E.; Robb, M. A.; Cheeseman, J. R.; Scalmani, G.; Barone, V.; Mennucci, B.; Petersson, G. A.; Nakatsuji, H.; Caricato, M.; Li, X.; Hratchian, H. P.; Izmaylov, A. F.; Bloino, J.; Zheng, G.; Sonnenberg, J. L.; Hada, M.; Ehara, M.; Toyota, K.; Fukuda, R.; Hasegawa, J.; Ishida, M.; Nakajima, T.; Honda, Y.; Kitao, O.; Nakai, H.; Vreven, T.; Montgomery, J. A.; Peralta, J. E.; Ogliaro, F.; Bearpark, M.; Heyd, J. J.; Brothers, E.; Kudin, K. N.; Staroverov, V. N.; Keith, T.; Kobayashi, R.; Normand, J.; Raghavachari, K.; Rendell, A.; Burant, J. C.; Iyengar, S. S.; Tomasi, J.; Cossi, M.; Rega, N.; Millam, J. M.; Klene, M.; Knox, J. E.; Cross, J. B.; Bakken, V.; Adamo, C.; Jaramillo, J.; Gomperts, R.; Stratmann, R. E.; Yazyev, O.; Austin, A. J.; Cammi, R.; Pomelli, C.; Ochterski, J. W.; Martin, R. L.; Morokuma, K.; Zakrzewski, V. G.; Voth, G. A.; Salvador, P.; Dannenberg, J. J.; Dapprich, S.; Daniels, A. D.; Farkas, O.; Foresman, J. B.; Ortiz, J. V.; Cioslowski, J.; Fox, D. J. *Gaussian 09, Revision B.01*; Gaussian, Inc.: Wallingford, CT, 2010.
- (31) Guest, M. F.; Bush, I. J.; van Dam, H. J. J.; Sherwood, P.; Thomas, J. M. H.; van Lenthe, J. H.; Havenith, R. W. A.; Kendrick, J. *Mol. Phys.* **2005**, *103*, 719.
- (32) Lazzarretti, P.; Zanasi, R. *SYSMO package*; University of Modena: 1980. Additional routines by P. W. Fowler, E. Steiner, R. W. A. Havenith, A. Soncini.